

Chimeric mRNA-based COVID-19 vaccine induces protective immunity against Omicron and Delta variants

Qidong Hu,^{1,2} Ying Zhao,^{1,2} Namir Shaabani,^{1,2} Xiaoxuan Lyu,^{1,2} Colin Powers,^{1,2} Haotian Sun,¹ Vincent Cruz,¹ Karen Stegman,¹ Jia Xu,¹ Amber Fossier,¹ Yu Huang,¹ Giang Ho,¹ Yi Kao,¹ Zhihao Wang,¹ Zhenping Wang,¹ Yue Hu,¹ Yi Zheng,¹ Lilian Kyaw,¹ Cipriano Zuluaga,¹ Hua Wang,¹ Hong Pei,¹ Robert Allen,¹ Hui Xie,¹ Henry Ji,¹ and Runqiang Chen¹

¹Sorrento Therapeutics Inc., 4955 Directors Place, San Diego, CA 92121, USA

The emerging SARS-CoV-2 variants of concern (VOCs) exhibit enhanced transmission and immune escape, reducing the effectiveness of currently approved mRNA vaccines. To achieve wider coverage of VOCs, we first constructed a cohort of mRNAs harboring a furin cleavage mutation in the spike (S) protein of predominant VOCs, including Alpha (B.1.1.7), Beta (B.1.351), Gamma (P.1), and Delta (B.1.617.2). The mutation abolished the cleavage between the S1 and S2 subunits. Systematic evaluation in vaccinated mice discovered that individual VOC mRNAs elicited strong neutralizing activity in a VOC-specific manner. In particular, the neutralizing antibodies (nAb) produced by immunization with Beta-Furin and Washington (WA)-Furin mRNAs showed potent cross-reactivity with other VOCs. However, neither mRNA elicited strong neutralizing activity against the Omicron variant. Hence, we further developed an Omicron-specific mRNA vaccine that restored protection against the original Omicron variant and some sublineages. Finally, to broaden the protection spectrum of the new Omicron mRNA vaccine, we engineered an mRNA-based chimeric immunogen by introducing the receptor-binding domain of Delta variant into the entire S antigen of Omicron. The resultant chimeric mRNA induced potent and broadly nAbs against Omicron and Delta, which paves the way to developing new vaccine candidates to target emerging variants in the future.

INTRODUCTION

The global pandemic caused by the severe acute respiratory syndrome coronavirus 2 (SARS-CoV-2) has already claimed millions of lives since the outbreak in January 2020.¹ Numerous strategies have been employed to combat the spread of this infectious disease by public health agencies worldwide. As one of the most widely adopted approaches, vaccination has been proved to be a key tool for tackling COVID-19. To date, there are a total of eleven COVID-19 vaccines granted for emergency use or fully approved globally.² Among the various types of vaccine platforms, the mRNA vaccine has been proved to be effective against COVID-related hospitalization and death.

Despite these efforts, the pandemic continues to pose a threat to public health due to the constant viral evolution and the consequential emergence of new SARS-CoV-2 variants of concern (VOCs).³ Hence, there is an urgent need to develop more efficacious mRNA vaccines to fight against the current and potentially future VOCs.

The designated VOCs have caused multiple waves of widespread outbreak with unprecedented speed. Back in 2020, the first VOC Alpha (B.1.1.7) was detected in the United Kingdom, leading to more than 100,000 confirmed cases in the country. Following the emergence of Alpha variant, there were two other outbreaks originating from South Africa and Brazil, triggered by the Beta (B.1.351) and Gamma (P.1) variants, respectively.^{1,3,4} With additional mutation in spike (S) protein, both VOCs were estimated to be 40%–80% more transmissible than the wild-type lineage. Furthermore, the Beta variant exhibits great immune escape, and COVID-19 vaccination only showed 75% effectiveness against infection.⁵ In late 2020, a new variant B.1.617.2 (Delta) was identified and subsequently contributed to a surge in cases in India and worldwide shortly afterward. Besides the increased transmissibility, Delta variant has been shown to cause more severe disease and result in a poorer prognosis than previously reported VOCs.^{6–8} To make things even worse, the effectiveness of existing mRNA vaccines against Delta has dropped considerably, from ~95% for the original Washington (WA) strain to 76% (mRNA-1273) and 42% (BNT162b2).⁹ By June 2021, global COVID-19-related deaths hit 5 million as Delta variant swept over 161 countries around the world.

More recently, the WHO declared a novel VOC B.1.1.529, designated as Omicron (BA.1), on November 26, 2021, only 2 days after it was first reported to the WHO by South Africa.¹⁰ Omicron quickly

Received 18 March 2022; accepted 31 October 2022;
<https://doi.org/10.1016/j.omtn.2022.10.021>.

²These authors contributed equally

Correspondence: Sorrento Therapeutics Inc., 4955 Directors Place, San Diego, CA 92121, USA.

E-mail: rchen@sorrentotherapeutics.com



outcompeted the circulating Delta variant within weeks after landing in Europe and the United States, and has become the dominant VOC around the globe. Scientists found that there was a significant reduction in Omicron virus-neutralizing activity in sera obtained from individuals infected by pre-Omicron variants and populations vaccinated with immunogens based on early WA-1 virus.^{11–13} A huge number of breakthrough infections have been reported even from individuals fully vaccinated with the third booster shot. Although still largely effective in preventing hospitalization and mortality, the two existing mRNA-based vaccines have shown declining capabilities in preventing infection by various VOCs, especially Omicron. A plausible explanation for the increasingly large gap in vaccine coverage is that both fully approved mRNA vaccines encode the S protein of the original WA strain as the immunogen.

Compared with its ancestral strain, Omicron contains more than 30 additional mutations within the S protein coding sequence, 15 of which reside in the receptor-binding domain (RBD).¹⁴ Capable of binding to the human angiotensin-converting enzyme 2 (ACE2) receptor, the RBD has been demonstrated by pioneering structural analysis to be the key domain for virus attachment and entry to human cells.¹⁵ Thus, the high rate of mutations in Omicron RBD may dramatically alter the interaction dynamics between the virus and host cell, which could, at least partially, explain the enhanced transmissibility and breakthrough cases.^{4,13}

In the present study, we explored various strategies to develop new mRNA vaccines that can provide broad and effective protection against predominant SARS-CoV-2 VOCs. We first screened five monovalent mRNA vaccines encoding the S protein of Alpha, Beta, Gamma, Delta, and the original WA strain. All the vaccines harbor the mutation that abolishes the furin-mediated cleavage between S1 and S2 domains of S protein. It was found that Beta-Furin and WA-Furin mRNAs showed the most potent cross-neutralizing activity against other VOCs, except for Omicron. Hence, we further constructed the mRNA vaccine encoding the S protein of Omicron, which was shown to induce the strongest protection against Omicron. However, it did not elicit broad neutralizing capacity against other VOCs, such as Delta. To address the observed limitations of an Omicron-specific mRNA vaccine, we developed a chimeric mRNA by incorporating an extra RBD from Delta variant in the context of the S protein of Omicron. The resultant chimeric mRNA vaccine elicited significantly higher cross-neutralization activity against Delta while retaining efficacy against Omicron. Our findings thus provide insights into the development of the next generation of mRNA vaccine with wider coverage of possible future VOCs of SARS-CoV-2, and the potential to provide vaccine coverage for respiratory pathogens outside of the family Coronaviridae.

RESULTS

mRNA vaccine harboring furin cleavage mutation elicits strong neutralizing titers and T cell responses

Previously, we have designed a SARS-CoV-2 S mRNA vaccine that achieves high expression in mammalian cells.¹⁶ This mRNA vaccine

encodes the S protein from the Wuhan/Washington (WA) strain and contains a polybasic furin cleavage site at the junction of S1 and S2 subunits. The feature could affect the stability of spike protein and reduce the pool of antigenic epitopes available to induce cellular and humoral immunity.¹⁷ In addition, cleaved S1 was detected in the blood of immunized subjects receiving existing mRNA vaccine,¹⁸ raising a significant question of whether this free moiety could represent a potential safety issue by mimicking full-length S protein to activate ACE2 and thus trigger some side effects, including myocarditis in healthy subjects. Thus, to further optimize the mRNA vaccine and eliminate these potential safety concerns, the furin cleavage site between the S1 and S2 domains of the spike was mutated (Figure 1A) in the currently reported build of our mRNA vaccine candidates.

We then constructed two sets of mRNAs encoding the S protein of all the predominant SARS-CoV-2 VOCs, one with the wild-type (WT) furin cleavage site and the other with mutated site. We examined and compared the expression of these VOC mRNAs, including WA, Alpha, Beta, Gamma, and Delta, in 293T cells. The flow cytometry results showed that removal of the furin cleavage site increased the surface expression of VOC S protein in transfected 293T cells (Figures 1B and S1), and Western blot confirmed that the mutation abolished the furin cleavage and lowered the level of free S1 in the conditioned medium (Figures 1C and 1D). We thus hypothesized that the boosted expression of the furin mutant could result in stronger immunogenicity. To test the hypothesis, WA WT or furin-mutant mRNAs were formulated with an in-house lipid nanoparticle (LNP), and 6-week-old female BALB/c mice were intramuscularly injected with two doses of 5.0 µg of LNP mRNA separated by 3 weeks. ELISA on the sera collected 14 days after booster revealed that mRNA carrying the furin cleavage mutation elicited an average endpoint titer (EPT) of total binding antibody comparable with its WT version (Figure S2A). We then performed the plaque reduction neutralization test (PRNT) using the same antisera to assess neutralizing antibody (nAb).^{19,20} Consistent with ELISA data, PRNT results indicated that the neutralizing activity of sera from WA-Furin mutant-injected mice (Figure S2B) was comparable with that measured in mice vaccinated with the WT version.

To confirm that the furin cleavage mutation would not compromise the immunogenicity of spike mRNA vaccine, 6-week-old female BALB/c mice were immunized twice with 0.2 µg, 1.0 µg, or 5.0 µg of WA or WA-Furin mRNA LNP. Five weeks after the booster injection, splenocytes were isolated and stimulated with the peptide pool that covers the S1 subunit of the S protein. Intracellular cytokine staining showed that WA and WA-Furin mRNAs elicited a comparable dose-dependent T_H1 response as exemplified by interferon-γ (IFN-γ) and tumor necrosis factor α (TNF-α), with limited T_H2 response indicated by interleukin-4 (IL-4) and IL-5 (Figures 2A and 2B). The mRNAs also triggered a potent induction of IFN-γ and TNF-α expression in CD8⁺ T cells in a dose-dependent manner (Figures 2A and 2B). We then evaluated the sera from immunized mice for neutralizing activity against pseudotyped WA virus. The neutralization assay confirmed that furin cleavage mutation did not

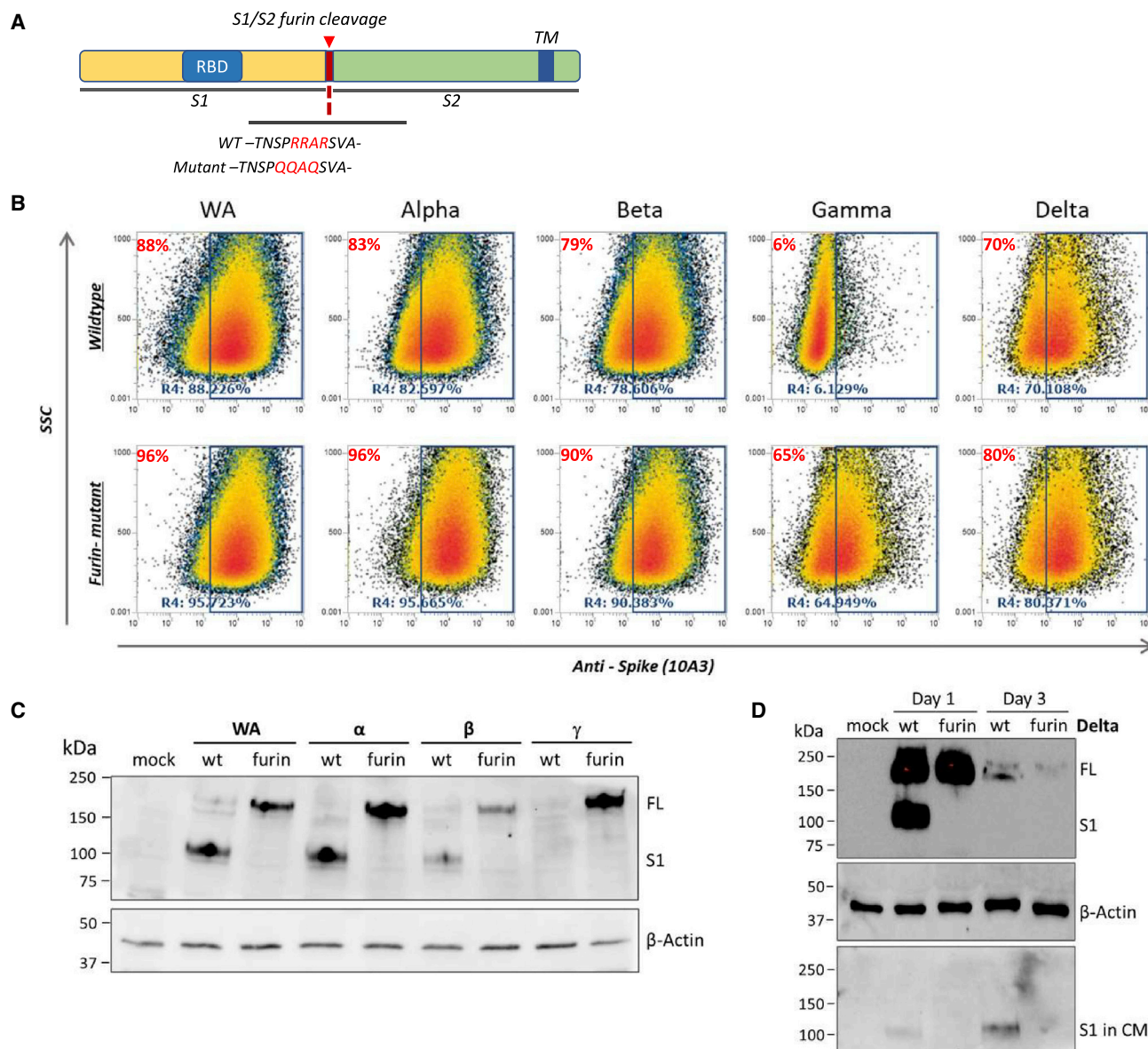


Figure 1. Expression and cleavage of furin cleavage mutant mRNA

(A) Design of the furin cleavage mutant mRNA. (B) 293T cells in a 24-well plate were transfected with 1 μ g of indicated variant mRNAs and collected 72 h post transfection. The surface expression of spike was assessed by flow cytometry using the proprietary anti-spike 10A3 antibody. $n = 3$. (C) 293T cells in a 6-well plate were transfected with 5 μ g of indicated variant mRNAs. The cell lysates were collected 24 h post transfection and analyzed by Western blot using anti-S1 antibody. (D) 293T cells in a 6-well plate were transfected with 5 μ g of wild-type or furin cleavage mutant spike mRNA of Delta variant. The cell lysate and CM were collected at day 1 and day 3 post transfection. The relative abundance of FL spike and free S1 was examined by Western blot. TM, transmembrane domain; FL, full-length S protein; CM, conditioned medium.

affect the immunogenicity of the mRNA vaccine at the doses tested (Figure S3). Hence, we incorporated the furin cleavage mutation in the following studies.

Next, to investigate the ability of individual SARS-CoV-2 VOC mRNA vaccines to generate nAb and to profile their coverage spectrum *in vivo*, we immunized 6-week-old female BALB/c mice with LNP-encapsulated furin-mutant VOC mRNAs and compared the

performance of individual mRNAs in vaccinated mice. The EPT of total binding antibodies was first measured by ELISA using the sera at day 14 post two-dose injection. As expected, each mRNA induced the strongest Ab response against the corresponding VOC S protein, with the exception of Gamma (Figure 3A). To analyze the neutralizing capability of individual sera, PRNT was performed whereby VeroE6 cells were exposed to the live virus of five VOCs in the absence or presence of diluted serum collected from the immunized

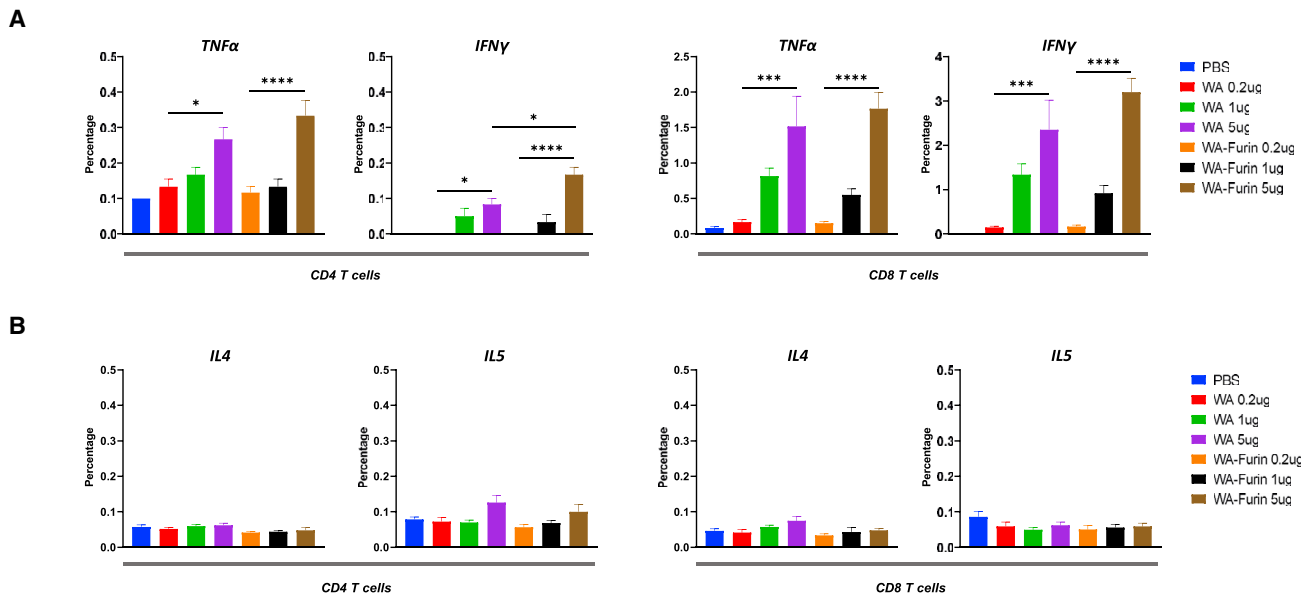


Figure 2. T_H1-biased immune response in vaccinated mice

Six-week-old female BALB/c mice were immunized twice with WA or WA-Furin-mutant mRNA with a 3-week interval. Five weeks after boost, splenocytes were stimulated *ex vivo* with the S1 peptide pool for 6 h. Intracellular cytokine staining was then performed to measure T_H1-related TNF- α and IFN- γ (A), and T_H2-related IL-4 and IL-5 (B). Error bars: mean \pm SEM; n = 6. *p < 0.05, ***p < 0.001, ****p < 0.0001 by one-way ANOVA followed by Tukey's test.

mice. In keeping with the ELISA results, the experiment showed that the VOC-specific strategy using individual monovalent mRNA vaccines generally provided variant-specific protection (Figure 3B). Based on the dilution factors at 50% neutralization, vaccination with some VOC mRNAs, especially Beta-Furin, was able to trigger a broad and potent immune response to the genetically divergent set of SARS-CoV-2 variants tested (Figure S4).

To confirm that Beta-Furin mRNA elicited an immune response in a similar manner to WA-Furin mRNA, Balb/c mice received two injections of WA-Furin or Beta-Furin mRNA at 0.2 μ g, 1.0 μ g, and 5.0 μ g. Five weeks after the booster injection, we first analyzed the T cell-based immunity by stimulating isolated splenocytes with the S1 peptide pool. Intracellular cytokine staining showed that both mRNAs elicited a dose-dependent T_H1 response as exemplified by IFN- γ and TNF- α , with limited T_H2 response indicated by IL-4 and IL-5 (Figures S5A and S5B). The mRNAs also triggered a potent induction of IFN- γ and TNF- α expression in CD8⁺ T cells in a dose-dependent manner (Figures S5A and S5B). We then assessed the effect of both mRNA vaccines on T cell composition and formation of memory B cells (Figure S6). The percentage of CD4⁺ T cells and CD8⁺ T cells showed minimal changes after vaccination. Interestingly, WA-Furin mRNA specifically increased the percentage of CD19⁺ memory B cells in the blood and spleen.

mRNA vaccines carrying furin cleavage mutation produce robust protection *in vivo*

The K18-hACE2 transgenic model has been extensively utilized to evaluate the vaccine efficacy and effectiveness in preventing COVID-19 in

the preclinical setting.^{21–24} Two key metrics to determine the severity of pathogenesis are the virus titer in the lung tissue and body-weight loss following virus infection. To investigate the protection capacity of our furin-mutant mRNA vaccines, K18-hACE2 mice were first intramuscularly administered with 5 μ g of WA-Furin or Beta-Furin mRNA twice with a 3-week interval. Five weeks post full vaccination, the animals were challenged with 1×10^5 half-maximal tissue culture infectious dose (TCID₅₀) of the WA, Beta, or Lambda variants (Figure 4A). Virus replication in the lung was then quantified to determine the effect of vaccination. The average virus titer was approximated to 1×10^6 , 2.1×10^5 , and 4.5×10^6 TCID₅₀/g for WA, Beta, and Lambda strains, respectively in the control group injected with PBS. On the other hand, immunization with either WA-Furin or Beta-Furin mRNA completely inhibited the replication of virus in the lungs, with virus titers falling below the limit of detection (Figure 4B). As expected, animals treated with PBS experienced dramatic weight loss in all challenge settings. The average body weight in the PBS controls declined to 82%, 78%, and 81% on day 5 post infection with WA, Beta, and Lambda strains, respectively. In contrast, none of the mice immunized with Beta-Furin or WA-Furin vaccines showed any sign of weight loss after infection for up to 5 days (Figure 4C). In addition, both furin-mutant mRNAs gave effective protection against the Lambda variant although the corresponding spike mRNA was not included among the immunogens, suggesting broad protection capacity of some VOC mRNAs.

Omicron variant undermines the effectiveness of the past VOC-based vaccines

In November 2021, a new SARS-CoV-2 variant, B.1.1.529 (Omicron), was identified in South Africa and declared as VOC by the WHO due

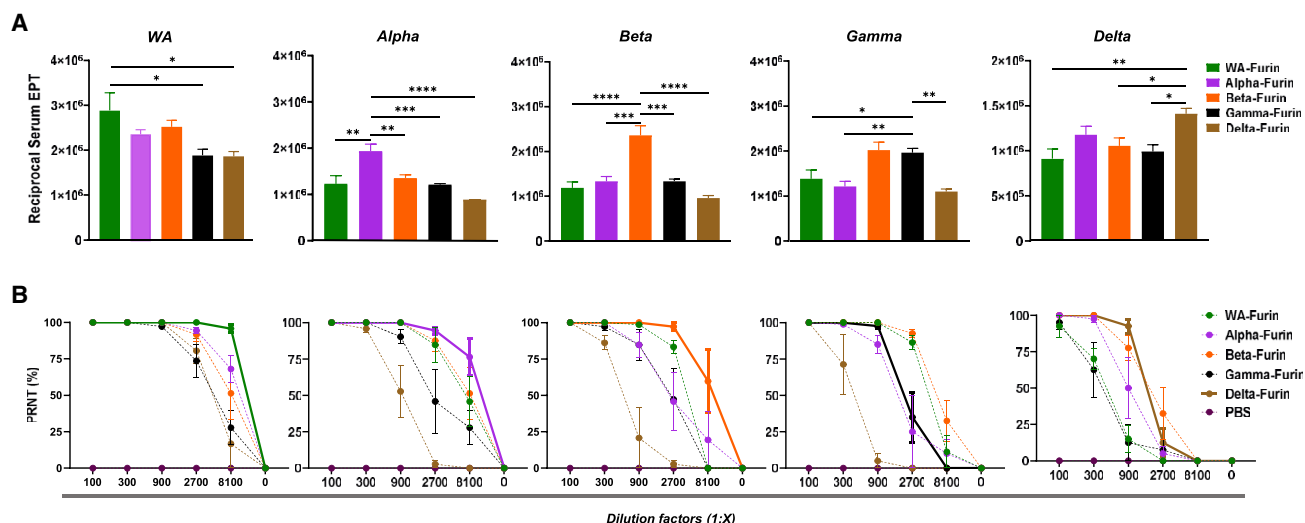


Figure 3. Antibody responses upon immunization with VOC-based vaccines *in vivo*

Six-week-old female BALB/c mice were immunized twice with indicated furin-mutant VOC mRNAs with a 3-week interval. (A) Sera at day 14 post booster were evaluated for antibodies binding to recombinant S protein from designated VOCs by ELISA. (B) Sera at day 14 post booster were evaluated for nAb responses against designated live virus by 50% plaque reduction neutralization test (PRNT). EPT, endpoint titer. Plots: mean \pm SEM; n = 4. *p < 0.05, **p < 0.01, ***p < 0.001, ****p < 0.0001 by one-way ANOVA followed by Dunnett's test.

to its rapid rise in global prevalence. Bearing an unusually large number of previously unreported RBD mutations as compared with other VOCs, Omicron exhibited the most significant escape from the serum of both fully vaccinated subjects and convalescents.²⁵ To investigate whether our optimized mRNA vaccines could offer effective protection against Omicron, vesicular stomatitis virus (VSV) pseudotyped viruses were used to determine the neutralization potency of sera collected from vaccinated animals. In agreement with other studies,²⁶ we found that the mean neutralization titer (IC_{50}) of Omicron was only 318 for the sera collected at day 14 after booster with WA-Furin mRNA, which represents a significant decrease of neutralization, as compared with WA pseudotyped virus with an IC_{50} of 16,194 (Figure S7). A similar decrease in the protection capacity against Omicron was observed for the sera from mice vaccinated with other VOC mRNAs (Figure S7). Even Beta-Furin mRNA, which has been shown to provide the broadest immune response against all major past VOCs (Figure 3), failed to induce sufficient protection against Omicron, prompting us to explore further immunogen designs to overcome this liability.

To establish the potential of a variant-matched monovalent vaccine to provide protective immunity against Omicron, we replaced the coding sequence of the original WA-Furin mRNA vaccine with Omicron S retaining the furin cleavage mutation. More than 85% of the Omicron-Furin mRNA transfected 293T cells, but not the mock control, could be detected by flow cytometry with Fc-tagged ACE2 recombinant protein (Figure S8). We then performed *in vivo* studies to assess the immunogenicity and efficacy of the Omicron-specific mRNA vaccine. BALB/c mice were immunized intramuscularly with 5 μ g of Omicron-LNP

mRNA, WA-LNP mRNA, or Beta-LNP mRNA two times at a 3-week interval. Serum was collected 2 weeks post booster. By using the recombinant Omicron S protein as the coating antigen in ELISA, high titers of binding antibodies were observed only in the sera of Omicron mRNA-injected mice (Figure 5A). By using pseudotyped Omicron virus in neutralization assay, we confirmed that the sera collected from Omicron mRNA-immunized animals offered superior protection against the infection of Omicron strain (Figure 5B), demonstrating that this newly designed mRNA vaccine could induce potent production of Omicron-specific nAbs *in vivo*. In the live virus PRNT, the sera collected 2 weeks after booster from Omicron mRNA-injected mice demonstrated stronger protection against Omicron infection than those from the Beta mRNA cohort (Figure S9).

To characterize the effect of vaccination on lymphocyte activation and proliferation, BALB/c mice were sacrificed 12 days after a single dose of Omicron mRNA at 0.2 μ g, 1.0 μ g, or 5.0 μ g, and the draining lymph node (LN) at the injection site was analyzed by flow cytometry. We noticed a dose-dependent increase in total B cells, class-switching B cells, germinal center B cells, and plasma cells (Figure 5C). Interestingly, both immunoglobulin G2 (IgG2)⁺ and IgG1⁺ B cells were increased at a comparable rate, suggesting a coordinated T_H1-T_H2 response. Furthermore, the vaccination with Omicron mRNA greatly increased the number of total T cells, CD4⁺ cells, and CD8⁺ T cells (Figure S10). T follicular helper (Tfh) cells, including the ICOS⁺ and CXCR5/PD1⁺ subsets, were also dramatically increased by the vaccination, especially at the highest dose of 5 μ g (Figures 5C and S11), which could contribute to the B cell proliferation and class switching in the germinal center.

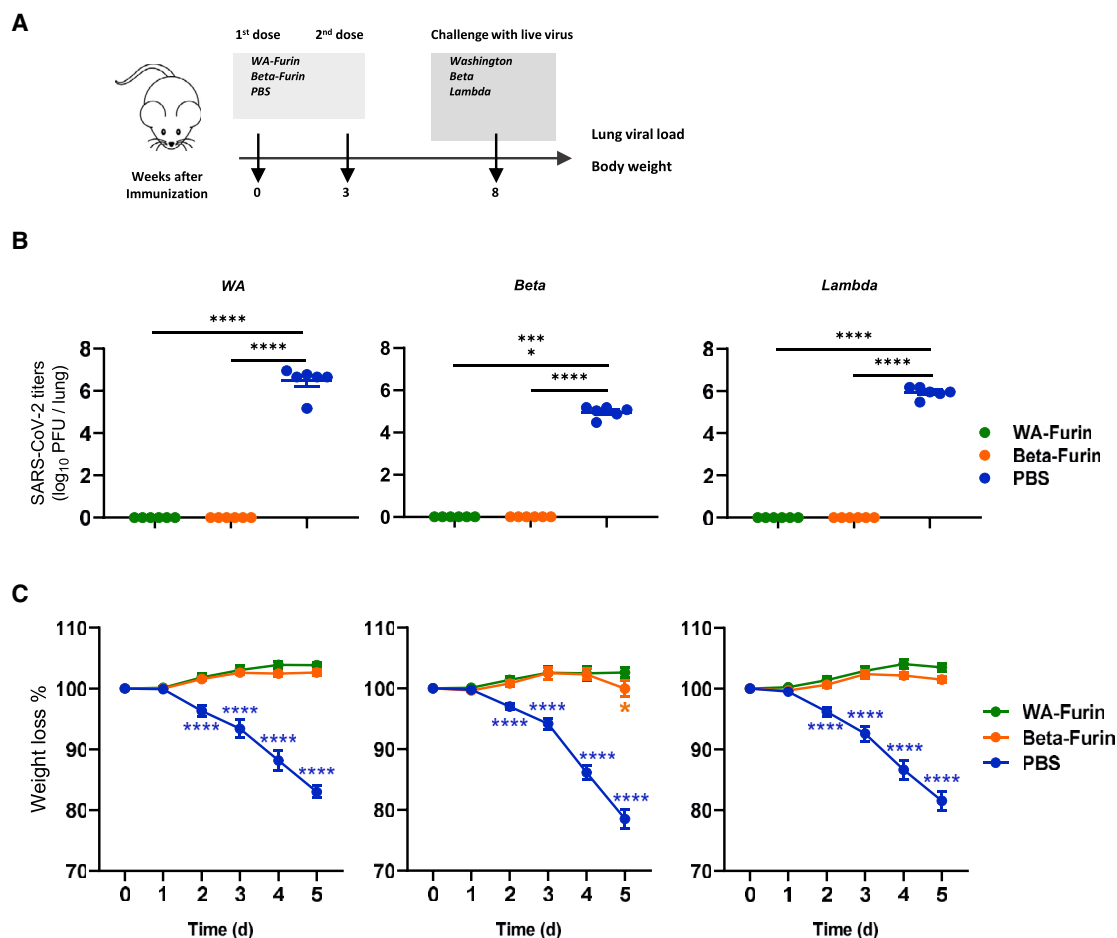


Figure 4. Immunization with furin cleavage mutant vaccine produces strong protection *in vivo*

(A) Schematic illustration of the *in vivo* study using K18 hACE2 mice. The lung virus titer (B) and body weight (C) were measured in mice challenged with the live virus of indicated SARS-CoV-2 VOCs after full immunization. Plots: mean \pm SEM; n = 6 (B) and n = 12 (C). *p < 0.05, ****p < 0.0001 by one-way ANOVA followed by Dunnett's test (B), or by two-way ANOVA followed by Dunnett's test (C).

To investigate whether Omicron mRNA can indeed elicit strong variant-specific immunity, K18 hACE2 mice were immunized with the mRNA at 0.2 μ g, 1.0 μ g, and 5.0 μ g twice at a 3-week interval. Five weeks after the booster injection the animals were challenged with the Omicron strain, and the virus titer in lungs was quantified 4 days later. Compared with control animals, no sign of viral replication was detected in Omicron mRNA-vaccinated mice, even at the lowest dose (Figure 5D), indicating strong immunity against this specific variant.

As the Omicron strain led to an increasing number of breakthrough cases even in fully vaccinated people, we wanted to investigate whether using Omicron-Furin mRNA solely as a boosting immunogen could provide enhanced protection. K18-ACE2 transgenic mice were immunized with two doses of Beta-Furin mRNA vaccines first, followed by the booster of PBS, 5 μ g of Beta-Furin, or 5 μ g of Omicron-Furin mRNA. Five weeks after the third dose, the animals were challenged with the Omicron virus. The quantification of virus

titers in lungs showed that the booster with either Beta-Furin or Omicron-Furin could indeed restore the immunity against Omicron (Figure 5E). To better simulate the real-world scenario, we set up another challenge study by administering two doses of WA-Furin mRNA into K18-ACE2 transgenic mice (Figure S12A). The animals then received the booster shot of either 5 μ g of WA-Furin mRNA or Omicron-Furin mRNA, and were challenged with live Omicron strain after 5 weeks. The quantification of virus loads showed that while the control group displayed high viral titer, up to 5×10^5 plaque-forming units (PFU) per lung, vaccinated mice showed no detectable viral replication in the lung (Figure S12B), suggesting that both WA-1 and Omicron-based booster mRNAs provided substantial and similar protection against Omicron.

Chimeric RBD-based mRNA vaccine elicits broad protection against Omicron and Delta

With the new Omicron mRNA vaccine, we sought to determine whether it could provide sufficient cross-reactive immunity against

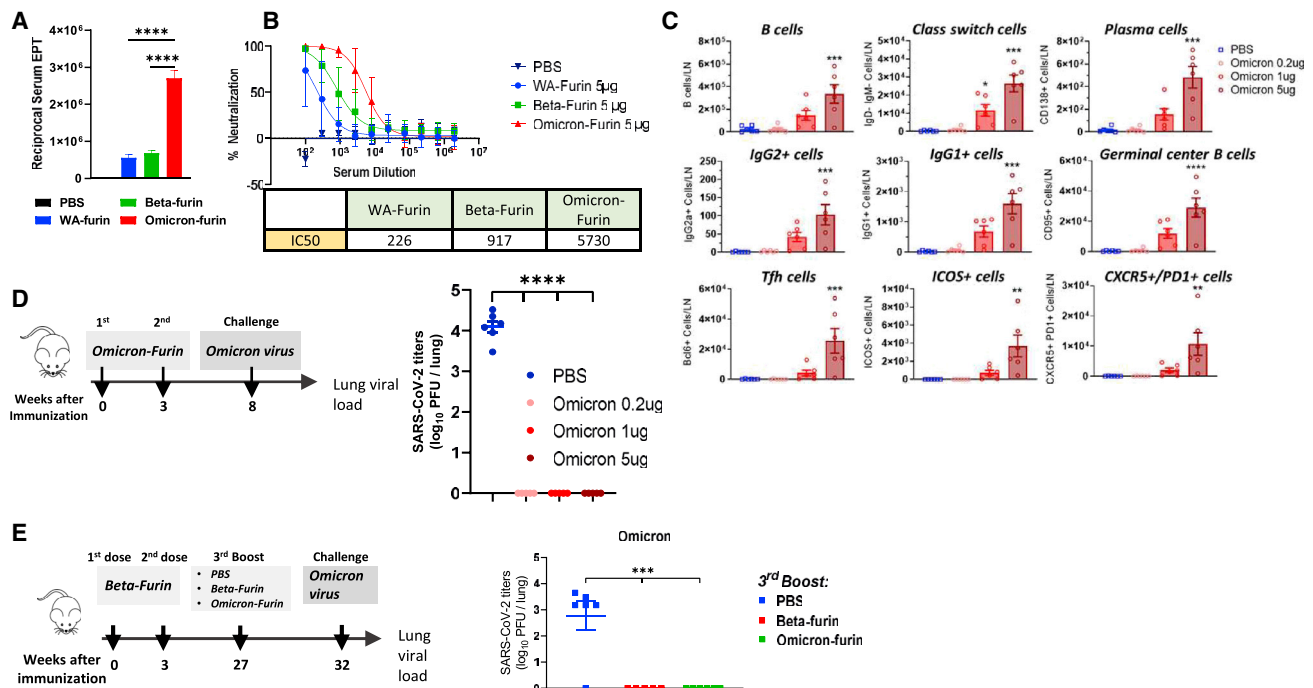


Figure 5. Immunization with Omicron-specific vaccine produces robust protection against Omicron challenge

BALB/c mice were intramuscularly injected with 5 μ g of Omicron-Furin, WA-Furin, or Beta-Furin mRNA twice. Sera at day 14 post booster were evaluated for total antibody binding to Omicron S protein by ELISA (A) and for nAb responses to pseudotyped Omicron virus by neutralization assay (B). Plots: mean \pm SEM; $n = 6$. **** $p < 0.0001$ by one-way ANOVA followed by Dunnett's test. (C) BALB/c mice were injected with different doses of Omicron-Furin mRNA. Twelve days post injection, the draining lymph nodes (LN) were collected and analyzed by flow cytometry for the abundance of indicated cell types. (D) K18 hACE2 mice were immunized with Omicron-Furin mRNA as illustrated (left panel). Five weeks after the booster injection, the animals were challenged with the Omicron live virus, and the lung virus titer was quantified after 4 days. (E) K18 hACE2 mice were immunized and boosted as illustrated (left panel). Five weeks after the third dose, the animals were challenged with the Omicron live virus, and the lung virus titer was quantified after 4 days. Plots: mean \pm SEM; $n = 6$. * $p < 0.05$, ** $p < 0.01$, *** $p < 0.001$, **** $p < 0.0001$ by one-way ANOVA followed by Dunnett's test. EPT, endpoint titer.

other VOCs. The ELISA and pseudovirus assays indicated that the Omicron-Furin mRNA vaccine elicited only limited immunity against other VOCs, such as Delta (Figure S13). Hence, in an effort to generate a vaccine with broad cross-reactivity against other VOCs, we constructed a chimeric VOC immunogen by inserting the RBD domain of the Delta variant directly upstream of the Omicron RBD within the Omicron spike backbone (Figure 6A). We first confirmed that the translation product of the chimeric mRNA could still bind to its natural receptor, ACE2, by flow cytometry (Figure S8). To evaluate the immunogenicity and efficacy of this chimeric design, mice were immunized twice with LNP-formulated mRNA as described above. The sera were collected 2 weeks following the second dose and analyzed for the titers of binding antibodies and nAbs against various VOCs. The ELISA results showed that compared with Delta mRNA, immunization with both chimeric Delta RBD-Omicron mRNA and original Omicron mRNA could generate high titers of Omicron S-binding antibodies; in addition, the chimeric mRNA outperformed the Omicron mRNA in the generation of binding antibodies against WA, Beta, Gamma, and Delta variants (Figure 6B). As the readout of ELISA assay is not a direct indicator of neutralizing capability, we used the same serum panel to further quantify the nAb titer against the pseudoviruses of Delta and three

Omicron subvariants (Figure 6C). The IC₅₀ of neutralization confirmed that compared with Delta-Furin mRNA, immunization with Omicron-Furin mRNA triggered significantly weaker immunity against Delta infection. Notably, when mice were immunized with the chimeric Delta RBD-Omicron mRNA, the sera provided fully restored protection against Delta infection. At the same time, the sera retained potent neutralizing activity toward not only the original Omicron (BA.1) but also sublineages including R346K and the more transmissible BA.2 (Figure 6C). The absolute IC₅₀ was 5,595 with Omicron-Furin and 4,945 with Delta RBD-Omicron against the ancestral Omicron strain, while the corresponding readout remained comparable at 5,232 and 5,138 against BA.2, respectively. Taken together, this chimeric design offers a powerful strategy to develop mRNA vaccines with broad protection capacity against COVID-19 and other infectious diseases.

DISCUSSION

Prophylactic nucleic acid vaccines can deliver the nucleotide sequence that codes for virus-derived but nonpathogenic proteins into host cells, thus mimicking a native infection to elicit an immune response. Unlike DNA, mRNA vaccines eradicate the need for nucleic acid to enter the nucleus to achieve expression, and they are less likely to

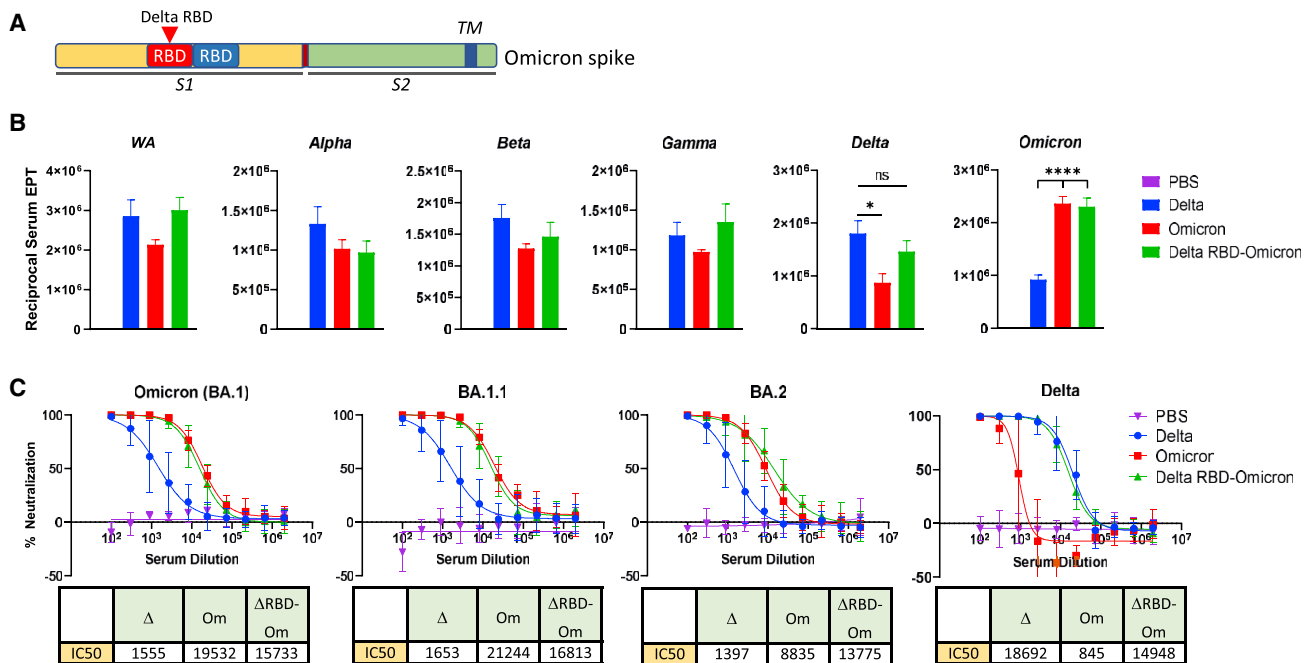


Figure 6. Delta RBD-Omicron immunization induces potent and broad neutralization activity against SARS-CoV-2 variants

(A) The schematic design of chimeric Delta RBD-Omicron mRNA. BALB/c mice were immunized with the indicated mRNA twice with a 3-week interval. The Day 14 sera post booster were evaluated for total binding antibodies specific to the S proteins of designated VOCs by ELISA (B) and for nAb responses to the indicated SARS-CoV-2 variants by pseudovirus assay (C). Plots: mean \pm SEM; n = 6. *p < 0.05, ****p < 0.0001 by one-way ANOVA followed by Dunnett's test. EPT: endpoint titer.

be integrated into the host genome. There are currently two mRNA-based SARS-CoV-2 vaccines authorized by the Food and Drug Administration (FDA) and widely disseminated. These vaccines encode for the S protein, the major surface protein on the coronavirus virion responsible for anchoring onto target cells, and thus the predominant virus-encoded target for nAb elicited by natural infection. Although clinical trials and real-world data have affirmed the safety and effectiveness of these FDA-authorized COVID-19 vaccines, more and more breakthrough infections have been reported for predominant VOCs. For example, the effectiveness of BNT162b2 against Delta-caused infection plummeted to 42% as compared with 95% against the ancestral WA strain,⁹ highlighting the need to develop vaccines that can offer wide protection against persistently emerging VOCs.

As each VOC possesses its unique set of mutations in the S protein, this will invariably result in distinct pools of epitopes being presented to lymphocytes by antigen-presenting cells (APCs). Hence, we first evaluated the protection conferred following vaccination with mRNA vaccines encoding the S proteins of VOCs that emerged prior to Omicron. Our *in vitro* and *in vivo* data clearly demonstrated the premise that the strongest immunity against individual VOCs can be achieved by vaccination with variant-specific mRNA. For example, immunization with Delta S mRNA provided the best protection against Delta, but not to other VOCs (Figure 3). We also noticed that WA and Beta mRNA, especially the latter, provided the widest breadth of coverage for other

VOCs. This could be explained by some mutations within Beta S protein, especially in the N terminus and RBD. These mutations are also present in other VOCs, for example, L18, K417, E484, N501, and D614, some of which are known to cause great immune escape.²⁷ Interestingly, Beta S mRNA has also been selected by Moderna to test in phase II trial either as a monovalent antigen or by mixing with mRNA-1273 to tackle the emerging VOCs.^{28,29}

With the emergence and rampage of Omicron during the course of our candidate vaccine development, we further tested the effectiveness of non-Omicron VOC mRNA vaccines against this new variant. Not surprisingly, none of these candidates induced strong immunity when challenged with Omicron (Figure S7). This could be explained by the more than 30 mutations in the S protein of Omicron, a mutational burden which far exceeded that of preceding VOCs. This observation is consistent with the complete escape of Omicron from most of emergency use authorization-approved neutralizing Ab and convalescent sera therapies.³⁰ To recapitulate our previous observation that VOC-matched vaccine induces the strongest nAb response in a VOC-dependent manner, we constructed a new mRNA vaccine encoding the S protein of Omicron, which indeed provided superior protection against the original BA.1 (Figures 5A and 5B) as well as the more recent BA.1.1 and BA.2 subvariants of Omicron (Figure 6C). The notion was reciprocally confirmed by the observation that Omicron mRNA did not induce strong immunity against other VOCs (Figure S13).

As the world is witnessing an astounding number of Omicron-related breakthrough cases even in fully vaccinated people who have received two doses of currently available mRNA vaccines, a serious concern has been raised of whether a booster is adequate to stop its spread. Hence, we compared Omicron-specific booster with WA-specific booster or Beta-specific booster to explore any additive protection. Our data strongly advocate the use of a third booster to restore strong immunity against Omicron; however, the heterologous booster scheme is not superior to boosting with the ancestral WA mRNA in terms of establishing immunity against Omicron (Figures 5E and S12). A similar conclusion was drawn by a research group from the National Institutes of Health, when they challenged mRNA-1273-vaccinated macaques with live Omicron virus.³¹ A plausible explanation is that although Omicron S protein has ~35 mutations, it still exhibits 97% similarity to the ancestral WA strain in the amino acid sequence. As a result, most of the epitopes presented to lymphocytes could remain the same, and the consequence of antigenic drift contributed by those ~35 mutations could be masked by the surge of nAbs generated after the third dose. Hence, individuals with prior immunity from vaccination may not necessarily benefit from a change in vaccinating antigens. Moreover, considering the cost and time needed to put variant-specific mRNA vaccine to practical use, the homologous booster scheme remains a scientifically proven and economically feasible option at hand in the fight against COVID-19.

Nonetheless, the concept of universal vaccine is still very appealing for at least two reasons. One is that the virus could keep accumulating more mutations to eventually nullify the effectiveness of existing mRNA vaccines. The other is that the idea can be applied to establish immunity against viruses causing different diseases. For example, dimeric RBDs have been ligated in tandem to target MERS, SARS, and COVID-19.³² In comparison, our chimeric design included the incorporation of the RBD of Delta variant in the Omicron S mRNA, which offers a larger pool of epitopes. Remarkably, we found that the resultant mRNA restored the strong protection against Delta infection while retaining the effective immunity against Omicron (Figure 6). Similar strategies have also been explored to target the *Sarbecovirus* subgenus with a single-molecule antigen,³³ suggesting broad applications of the chimeric vaccine design to deliver effective protection against a wide panel of diseases. Early this year, both Pfizer and Moderna launched clinical trials to evaluate the safety and efficacy of Omicron-based vaccines. While they have been shown to be safe and provide enhanced immunity against Omicron as compared with the WA-based vaccine, the concept of chimeric vaccine could offer an alternative to currently adopted monovalent design to offer both potent and broad protection, especially when facing the newly emerging subvariants of Omicron.

Another unique feature of our mRNA vaccine is the mutation of furin cleavage site between the S1 and S2 domains of S protein. This cleavage is believed to have emerged during viral transmission from its zoonotic host to humans and is one of the key attributes to explain the high transmissibility of SARS-CoV-2 in humans.³⁴ The mutation is mainly to address the concern that circulating S1 was detected in

the plasma of vaccinated subjects.³⁵ Although the clinical consequence of the free S1 moiety has not been fully established, studies have suggested that S1 can be taken up by many critical organs, such as liver, kidney, and spleen, and even cross the blood-brain barrier to gain access to the brain.³⁵ Hence, we mutated the furin cleavage site and confirmed the abrogation of S1 liberation in both the cell lysates and conditioned medium. Although a similar design was adopted in the recombinant protein-based NVX-CoV2373 by Novavax, it is not present in the two mRNA-based COVID-19 vaccines authorized by the FDA. Interestingly, an mRNA vaccine incorporating the furin cleavage mutation MRT5500 was already launched by Sanofi and Translate Bio, and is being evaluated in phase I/II trials (ClinicalTrials.gov: NCT04563702). Another potential benefit of furin cleavage mutation is that by retaining the full-length S protein within the cell and on the cell surface (Figures 1B–1D and S1), a larger pool of antigens could become available for presentation to induce adaptive immunity. Indeed, S protein with furin cleavage mutation was shown to bind with higher affinity to ACE2.³⁶

Taken together, our in-house-designed mRNA vaccine represents a potentially safer alternative to existing products on the market and can induce stronger immunity against past and current VOCs, including Delta and Omicron. Our chimeric design will also facilitate the development of next-generation vaccines that achieve the balance between effectiveness and coverage, not only for the variants of SARS-CoV-2 but also for other viruses.

MATERIALS AND METHODS

In vitro transcription and purification of RNA

To generate the template for RNA synthesis, the sequences of the SARS-CoV-2 S protein of VOC were codon optimized and cloned into pVAX1-based backbone which features 5' UTR, 3' UTR and poly(A) tail. To increase the protein stability, 2P mutations at positions 986–987 were introduced. The plasmid DNA was produced in bacteria, purified, and linearized by a single-site restriction enzyme digestion. The template DNA was purified, spectrophotometrically quantified, and *in vitro* transcribed by T7 RNA polymerase (cat. #M0251, NEB) in the presence of a trinucleotide cap1 analog, m7(3OMeG) (5')ppp(5') (2OMeA)pG (cat. #N-7113, TriLink), and of N1-methylpseudouridine-5'-triphosphate (cat. #N-1081, TriLink) in place of uridine-5'-triphosphate. After the reaction, DNase I (cat. #M0303, NEB) was added to remove the template DNA, and the mRNA was purified by LiCl precipitation (cat. #AM9480, Thermo Fisher).

mRNA formulation

LNPs were prepared by microfluidic mixing of a buffered solution of mRNA with an ethanol solution of lipids (distearoylphosphatidylcholine, cholesterol, 1,2-dimyristoyl-rac-glycero-3-methoxypolyethylene glycol 2000, and ionizable lipid). The ionizable lipid was screened and chosen by Sorrento Therapeutics. This unique ionizable lipid had an irreplaceable role in LNP mRNA delivery. At low pH during particle formation, the ionizable lipid with positively charged ionizable amine groups would interact with the anionic mRNA, forming the core of

the LNPs. The LNPs were concentrated by dialysis against an aqueous buffer system, following a 0.2- μ m sterile filtration. The LNPs were tested for mRNA concentration, encapsulation efficiency, particle size, pH, and osmolality.

***In vitro* mRNA expression**

With 293T adherent cells, mRNA (2.5 μ g) of WT versus mutant from five variants (Washington, Alpha, Beta, Gamma, and Delta) were transfected with Lipofectamine MessengerMAX Transfection Reagent (2 μ L) and cultured for 72 h at 37°C with 0.5 mL of Dulbecco's modified Eagle's medium (DMEM) with 10% fetal bovine serum (FBS) in each well of a 24-well cell-culture-treated plate. Transfected cells from each well were dislodged with 400 μ L of TrypLE at 72 h and neutralized with its own medium. Cell pellets were collected after spinning down at 550 \times g for 2 min by removing supernatant for each well.

Flow cytometry

The collected cell pellets were washed with 250 μ L of FACS buffer (Dulbecco's PBS + 0.5% BSA) in a 96-well treated plate followed by 30-min incubation with the in-house STI-2020 (for DCs) or 10A3 (for 293T cells) primary antibody (1:1,000) to detect SARS-CoV-2 S protein. FACS buffer (200 μ L) was used to wash the cells twice with the same speed and time after 30 min of incubation, followed by rat anti-human Fc antibody conjugated to APC (cat. #410712, BioLegend; 1:100 dilution) for 15 min on ice in darkness for secondary detection. The cells were spun down, then the pellets were washed twice with the same speed and time of centrifugation using 200 μ L of FACS buffer and resuspended in 200 μ L of FACS buffer. The fluorescent intensity of positive cells within the gated population was detected by an Attune NxT Flow Cytometer (Thermo Fisher) using 100 μ L of acquisition volume setting.

SARS-CoV-2 virus

SARS-CoV-2 viruses were obtained from BEI resources (Washington strain NR-52281; Alpha variant NR-54000; Beta variant NR-54009; Gamma variant NR-54982; Delta variant NR-55611 or NR-55672; Lambda variant NR-55654 and Omicron NR-56461). VeroE6 monolayers were infected at a multiplicity of infection of 0.01 in 5 mL of virus infection medium (DMEM + 2% fetal calf serum + 1 \times penicillin/streptomycin). Tissue culture flasks were incubated at 36°C and slowly shaken every 15 min for a 90-min period. Cell growth medium (35 mL) was added to each flask, and infected cultures were incubated at 36°C/5% CO₂ for 48 h. Medium was then harvested and clarified to remove large cellular debris by room-temperature centrifugation at 3,000 rpm.

Animals and *in vivo* studies

Six-week-old BALB/c female mice were purchased from The Jackson Laboratory. All protocols were approved by the Institutional Animal Care and Use Committee. mRNA formulations were diluted in 50 μ L of 1 \times PBS, and mice were inoculated intramuscularly into the same hindleg for both prime and booster. There was a 3-week interval between prime and booster. Two weeks after booster, mouse blood was

collected from retro-orbital for ELISA and pseudovirus neutralization assay.

ELISA

Ni-NTA HisSorb plates (Qiagen) were coated with 50 ng/well of S1 proteins (all from Sino Biological, cat. #40591-V08H, 40,589-V08B6, 40,589-V08B7, 40,589-V08B8, 40,589-V08B16) in 1 \times PBS at 4°C overnight. To block the plate, Blocker Casein (cat. #37528, Thermo Fisher) was used for 1 h at room temperature. After standard washes and blocks, plates were incubated with serial dilutions of sera for 1 h at room temperature. Following washes, goat anti-mouse IgG (H + L)-HRP conjugate (cat. #1721011, Bio-Rad) were used as secondary Abs, and a Pierce TMB substrate kit (cat. #34021, Thermo Fisher) was used as the substrate. The absorbance was measured at 450 nm using a BioTek Cytation 5 plate reader. Endpoint tiers were calculated as the dilution that emitted an optical density exceeding 4 \times background (secondary Ab alone).

T follicular helper and B cell phenotype detection in lymph node by flow cytometer

For mouse T cell and B cell analysis in lymphoid tissues, LN cells were stained for viability and extracellular antigens with directly labeled antibodies, CD95 (BioLegend 152606), IgD (BioLegend 405710), GL7 (BioLegend 144617), live/dead fixable yellow dead cell staining (Thermo Fisher Scientific L34968), CD19 (BioLegend 115555), biotinylated SARS-CoV-2-S1 protein (BioLegend 793804), anti-biotin (BioLegend 409003), CD3 (BioLegend 100220), CD3 (BioLegend 100204), CD4 (BioLegend 100540), ICOS (BioLegend 117420), CD8 (BioLegend 557654), CD45 (BioLegend 103134), CXCR5 (BioLegend 145504), PD-1 (BioLegend 135231), CD38 (BioLegend 102712), IgG1 (BioLegend 406620), and IgG2a (BioLegend 407114). Cells were washed, fixed, and permeabilized by using the Ebioscience Foxp3/Transcription Factor Staining Buffer Set (Thermo Scientific 00-5523-00) kit according to manufacture instructions. Permeabilized cells were intracellularly stained with Bcl-6 (BioLegend 358512). Cells were acquired on an Attune NxT Flow Cytometer and analyzed with Attune NxT software v.4.2.0.

Quantifying SARS-CoV-2 S-specific T cells in mice

Five weeks after booster, mouse splenocytes were isolated and incubated for 6 h at 37°C with BD GolgiPlug (BD Bioscience 555028) and with or without spike peptide pools (JPT Peptide Technologies PM-WCPV-S-1). Cells were washed, stained, and analyzed as described in the section "[T follicular helper and B cell phenotype detection in lymph node by flow cytometer.](#)" Antibodies for extracellular antigens are CD3 (BioLegend 100220), CD4 (BioLegend 100540), CD8 (BD Bioscience 557654), CD44 (BioLegend 103040), anti-I-A/I-E (BioLegend 107608), and live/dead fixable yellow dead cell staining (Thermo Scientific L34968), and for intracellular antigens are TNF- α (BioLegend 506304) and IFN- γ (BioLegend 505810).

Pseudovirus neutralization assay

SARS-CoV-2 S pseudotyped Δ G-VSV-luciferase was generated by nucleofection of BHK cells (maintained in DMEM/F12 with 10%

FBS and 5% tryptose phosphate broth) with S-expressing plasmid followed by transduction with G-pseudotyped Δ G-luciferase (G* Δ G-luciferase) rVSV (Kerafast) 18–24 h later. The supernatant containing pseudovirus was collected after 24 h and stored at -80°C . Pseudovirus was normalized for luciferase expression using G* Δ G-luciferase VSV of known titer as the standard. For neutralization testing, HEK-Blue 293 hACE2-TMPRSS2 cells (Invivogen; maintained in DMEM with 10% FBS) were plated to white-walled 96-well plates at 40,000 cells/well and incubated at $37^{\circ}\text{C}/5\% \text{CO}_2$. The next day, SARS-CoV-2 S pseudotyped Δ G-VSV-luciferase was incubated with a dilution series of mouse serum (dilutions as indicated) and anti-VSV-G (Kerafast; 1 $\mu\text{g}/\text{mL}$) antibody for 30 min at room temperature and added to the HEK-Blue 293 hACE2-TMPRSS2 cells. Transduced cells were incubated for 24 h at $37^{\circ}\text{C}/5\% \text{CO}_2$ and luminescence measured by addition of 40 μL of ONE-Glo reagent (Promega) with detection using a Tecan Spark plate reader. Percent inhibition was calculated using the formula $1 - ([\text{luminescence of serum treated sample}]/[\text{average luminescence of untreated samples}]) \times 100$. The average of quadruplicate samples was included in the analyses.

Plaque reduction neutralization test

Simian VeroE6 cells were plated at 18×10^3 cells/well in a flat-bottom 96-well plate in a volume of 200 μL /well. After 24 h, a serial dilution of seropositive blood serum was prepared in a 100 μL /well at twice the final concentration desired, and live virus was added at 1,000 PFU/100 μL of SARS-CoV-2 and subsequently incubated for 1 h at 37°C in a total volume of 200 μL /well. Cell culture medium was removed from cells and sera/virus premix was added to VeroE6 cells at 100 μL /well and incubated for 1 h at 37°C . After incubation, 100 μL of “overlay” (1:1 of 2% methylcellulose [Sigma] and culture medium) was added to each well and incubation commenced for 3 days at 37°C . Plaque staining using Crystal Violet (Sigma) was performed upon 30 min of fixing the cells with 4% paraformaldehyde (Sigma) diluted in PBS. Plaques were assessed using a light microscope (Keyence).

Challenge study

K18-hACE2 transgenic mice were purchased from The Jackson laboratory and maintained in pathogen-free conditions, with handling conforming to the requirements of the National Institutes of Health and the Scripps Research Institute Animal Research Committee. 8- to 12-week-old mice were injected with the indicated administration technique under isoflurane anesthesia in the right hind flank area for intramuscular injections. Mice were infected intranasally with 10,000 PFU of SARS-CoV-2 in a total volume of 50 μL .

Plaque assay

VeroE6 cells were plated at 3×10^5 cells/well in 24-well plates in a volume 400 μL /well. After 24 h the medium was removed, and serial dilution of homogenized lungs was added to Vero cells and subsequently incubated for 1 h at 37°C . After incubation, an overlay (1:1 of 2% methylcellulose [Sigma] and culture medium) was added

to each well and incubation commenced for 3 days at 37°C . Plaque staining was performed using Crystal Violet as mentioned above.

Statistics

Statistical significance of differences between experimental groups was determined with Prism software (GraphPad). All data are expressed as standard error of the mean (SEM). The statistical tests performed are indicated in the figure legends.

DATA AVAILABILITY

The authors confirm that the data supporting the findings of this study are available within the article and its [supplemental information](#). Raw data that support the findings of this study are available from the corresponding author upon reasonable request.

SUPPLEMENTAL INFORMATION

Supplemental information can be found online at <https://doi.org/10.1016/j.omtn.2022.10.021>.

ACKNOWLEDGMENTS

We thank Lisa Kerwin, Nancy Du, and Yanliang Zhang for providing reagents; Avery Coyle and Charlotte Sadaka for helpful discussions; and Brian Sun, Mike Ruse, Jr., Elizabeth Orr, Gali Steinberg-Tatman, and Maggy Smith for patent applications.

AUTHOR CONTRIBUTIONS

R.C., H.J., Q.H., Y. Z., N.S., X.L., and C.P. conceptualized and designed experiments. Q.H., Y. Z., N.S., X.L., C.P., H.S., V.C., K.S., J.X., A.F., Y. H., G.H., Y.K., Z. W., Y. H., Y. Z., L.K., C.Z., and H.W. performed experiments. Q.H., Y. Z., N.S., X.L., H.S., H.P., C.P., R.A., H.X., and R.C. analyzed and interpreted the data. Q.H., Y. Z., N.S., X.L., C.P., and R.C. wrote the paper.

DECLARATION OF INTERESTS

Sorrento authors own options and/or stock of the company. This work has been described in one or more provisional patent applications. H.J. is an officer at Sorrento Therapeutics, Inc.

REFERENCES

- Adam, D. (2022). The pandemic's true death toll: millions more than official counts. *Nature* 601, 312–315.
- WHO – COVID19 Vaccine Tracker <https://covid19.trackvaccines.org/agency/who/>, 2022.
- Otto, S.P., Day, T., Arino, J., Colijn, C., Dushoff, J., Li, M., Mechai, S., Van Domselaar, G., Wu, J., Earn, D.J.D., et al. (2021). The origins and potential future of SARS-CoV-2 variants of concern in the evolving COVID-19 pandemic. *Curr. Biol.* 31, R918–R929.
- Liu, Z., VanBlargan, L.A., Bloyet, L.-M., Rothlauf, P.W., Chen, R.E., Stumpf, S., Zhao, H., Errico, J.M., Theel, E.S., Liebeskind, M.J., et al. (2021). Identification of SARS-CoV-2 spike mutations that attenuate monoclonal and serum antibody neutralization. *Cell Host Microbe* 29, 477–488.e4.
- Abu-Raddad, L.J., Chemaitelly, H., and Butt, A.A. (2021). Effectiveness of the BNT162b2 covid-19 vaccine against the B.1.1.7 and B.1.351 variants. *N. Engl. J. Med.* 385, 187–189.
- Planas, D., Veyer, D., Baidaliuk, A., Staropoli, I., Guivel-Benhassine, F., Rajah, M.M., Planchais, C., Porrot, F., Robillard, N., Puech, J., et al. (2021). Reduced sensitivity of SARS-CoV-2 variant Delta to antibody neutralization. *Nature* 596, 276–280.

7. Mlcochova, P., Kemp, S.A., Dhar, M.S., Papa, G., Meng, B., Ferreira, I.A.T.M., Datir, R., Collier, D.A., Albecka, A., Singh, S., et al. (2021). SARS-CoV-2 B.1.617.2 Delta variant replication and immune evasion. *Nature* 599, 114–119.
8. Farinholt, T., Doddapaneni, H., Qin, X., Menon, V., Meng, Q., Metcalf, G., Chao, H., Gingras, M.-C., Farinholt, P., Agrawal, C., et al. (2021). Transmission event of SARS-CoV-2 delta variant reveals multiple vaccine breakthrough infections. Preprint at: medRxiv. <https://doi.org/10.1101/2021.06.28.21258780>.
9. Puranik, A., Lenehan, P.J., Silvert, E., Niesen, M.J.M., Corchado-Garcia, J., O'Horo, J.C., Virk, A., Swift, M.D., Halamka, J., Badley, A.D., et al. (2021). Comparison of two highly-effective mRNA vaccines for COVID-19 during periods of Alpha and Delta variant prevalence. Preprint at: medRxiv Prepr. Serv. Health Sci. <https://doi.org/10.1101/2021.08.06.21261707>.
10. Xu, Z., Liu, K., and Gao, G.F. (2022). Omicron Variant of SARS-CoV-2 Imposes a New Challenge for the Global Public Health (Biosaf. Health).
11. Cao, Y., Wang, J., Jian, F., Xiao, T., Song, W., Yisimayi, A., Huang, W., Li, Q., Wang, P., An, R., et al. (2021). Omicron Escapes the Majority of Existing SARS-CoV-2 Neutralizing Antibodies. p. 470392.
12. Lee, I.-J., Sun, C.-P., Wu, P.-Y., Lan, Y.-H., Wang, I.-H., Liu, W.-C., Tseng, S.-C., Tsung, S.-L., Chou, Y.-C., Kumari, M., et al. (2022). Omicron-specific mRNA Vaccine Induced Potent Neutralizing Antibody against Omicron but Not Other SARS-CoV-2 Variants.
13. Zhao, X., Li, D., Ruan, W., Zhang, R., Zheng, A., Qiao, S., Zheng, X., Zhao, Y., Chen, Z., Dai, L., et al. (2021). Reduced Sera Neutralization to Omicron SARS-CoV-2 by Both Inactivated and Protein Subunit Vaccines and the Convalescents.
14. Wu, L., Zhou, L., Mo, M., Liu, T., Wu, C., Gong, C., Lu, K., Gong, L., Zhu, W., and Xu, Z. (2022). SARS-CoV-2 Omicron RBD shows weaker binding affinity than the currently dominant Delta variant to human ACE2. *Signal Transduct. Target. Ther.* 7, 1–3.
15. Shang, J., Wan, Y., Luo, C., Ye, G., Geng, Q., Auerbach, A., and Li, F. (2020). Cell entry mechanisms of SARS-CoV-2. *Proc. Natl. Acad. Sci.* 117, 11727–11734.
16. Chen, R., Xie, H., Khorsandzadeh, S., Smith, M., Shaabani, N., Hu, Q., et al. (2022). Delivering an mRNA vaccine using a lymphatic drug delivery device improves humoral and cellular immunity against SARS-CoV-2 (*J Mol Cell Biol.*). <https://doi.org/10.1093/jmcb/mjac041>.
17. Peacock, T.P., Goldhill, D.H., Zhou, J., Baillon, L., Frise, R., Swann, O.C., Kugathasan, R., Penn, R., Brown, J.C., Sanchez-David, R.Y., et al. (2021). The furin cleavage site in the SARS-CoV-2 spike protein is required for transmission in ferrets. *Nat. Microbiol.* 6, 899–909.
18. Ogata, A.F., Cheng, C.-A., Desjardins, M., Senussi, Y., Sherman, A.C., Powell, M., Novack, L., Von, S., Li, X., Baden, L.R., et al. (2022). Circulating severe acute respiratory syndrome coronavirus 2 (SARS-CoV-2) vaccine antigen detected in the plasma of mRNA-1273 vaccine recipients. *Clin. Infect. Dis.* 74, 715–718.
19. Nyiro, J.U., Kiyuka, P.K., Mutunga, M.N., Sande, C.J., Munywoki, P.K., Scott, J.A.G., and Nokes, D.J. (2019). Agreement between ELISA and plaque reduction neutralisation assay in Detection of respiratory syncytial virus specific antibodies in a birth Cohort from Kilifi, coastal Kenya. *Wellcome Open Res.* 4, 33.
20. Schmidt, N.J., Dennis, J., and Lennette, E.H. (1976). Plaque reduction neutralization test for human cytomegalovirus based upon enhanced uptake of neutral red by virus-infected cells. *J. Clin. Microbiol.* 4, 61–66.
21. Radvak, P., Kwon, H.J., Kosikova, M., Ortega-Rodriguez, U., Xiang, R., Phue, J.-N., Shen, R.-F., Rozzelle, J., Kapoor, N., Rabara, T., et al. (2021). And B.1.351 Variants Are Highly Virulent in K18-ACE2 Transgenic Mice and Show Different Pathogenic Patterns from Early SARS-CoV-2 Strains, 447221.
22. Arce, V.M., and Costoya, J.A. (2021). SARS-CoV-2 infection in K18-ACE2 transgenic mice replicates human pulmonary disease in COVID-19. *Cell. Mol. Immunol.* 18, 513–514.
23. Dong, W., Mead, H., Tian, L., Park, J.-G., Garcia, J.I., Jaramillo, S., Barr, T., Kollath, D.S., Coyne, V.K., Stone, N.E., et al. (2021). The K18-human ACE2 transgenic mouse model recapitulates non-severe and severe COVID-19 in response to an infectious dose of the SARS-CoV-2 virus. *J. Virol.*
24. Winkler, E.S., Bailey, A.L., Kafai, N.M., Nair, S., McCune, B.T., Yu, J., Fox, J.M., Chen, R.E., Earnest, J.T., Keeler, S.P., et al. (2020). SARS-CoV-2 infection of human ACE2-transgenic mice causes severe lung inflammation and impaired function. *Nat. Immunol.* 21, 1327–1335.
25. Planas, D., Saunders, N., Maes, P., Guivel-Benhassine, F., Planchais, C., Buchrieser, J., Bolland, W.-H., Porrot, F., Staropoli, I., Lemoine, F., et al. (2022). Considerable escape of SARS-CoV-2 Omicron to antibody neutralization. *Nature* 602, 671–675.
26. Muik, A., Lui, B.G., Wallisch, A.-K., Bacher, M., Mühl, J., Reinholz, J., Ozhelvacı, O., Beckmann, N., Gümil Garcia, R. de la C., Poran, A., et al. (2022). Neutralization of SARS-CoV-2 Omicron by BNT162b2 mRNA vaccine-elicited human sera. *Science* 375, 678–680.
27. Winger, A., and Caspari, T. (2021). The spike of concern—the novel variants of SARS-CoV-2. *Viruses* 13, 1002.
28. Pajon, R., Doria-Rose, N.A., Shen, X., Schmidt, S.D., O'Dell, S., McDanal, C., Feng, W., Tong, J., Eaton, A., Maglinao, M., et al. (2022). SARS-CoV-2 omicron variant neutralization after mRNA-1273 booster vaccination. *N. Engl. J. Med.* *NEJMc2119912*.
29. Waltz, E. (2021). COVID vaccine makers brace for a variant worse than Delta. *Nature* 598, 552–553.
30. Liu, L., Iketani, S., Guo, Y., Chan, J.F.-W., Wang, M., Liu, L., Luo, Y., Chu, H., Huang, Y., Nair, M.S., et al. (2022). Striking antibody evasion manifested by the Omicron variant of SARS-CoV-2. *Nature* 602, 676–681.
31. Gagne, M., Moliva, J.L., Foulds, K.E., Andrew, S.F., Flynn, B.J., Werner, A.P., Wagner, D.A., Teng, I.-T., Lin, B.C., Moore, C., et al. (2022). mRNA-1273 or mRNA-Omicron Boost in Vaccinated Macaques Elicits Comparable B Cell Expansion, Neutralizing Antibodies and Protection against Omicron.
32. Dai, L., Zheng, T., Xu, K., Han, Y., Xu, L., Huang, E., An, Y., Cheng, Y., Li, S., Liu, M., et al. (2020). A universal design of betacoronavirus vaccines against COVID-19, MERS, and SARS. *Cell* 182, 722–733.e11.
33. Martinez, D.R., Schäfer, A., Leist, S.R., De la Cruz, G., West, A., Atochina-Vasserman, E.N., Lindesmith, L.C., Pardi, N., Parks, R., Barr, M., et al. (2021). Chimeric spike mRNA vaccines protect against Sarbecovirus challenge in mice. *Science* 373, 991–998.
34. Whittaker, G.R. (2021). SARS-CoV-2 spike and its adaptable furin cleavage site. *Lancet Microbe* 2, e488–e489.
35. Ogata, A.F., Cheng, C.-A., Desjardins, M., Senussi, Y., Sherman, A.C., Powell, M., Novack, L., Von, S., Li, X., Baden, L.R., et al. (2021). Circulating SARS-CoV-2 vaccine antigen detected in the plasma of mRNA-1273 vaccine recipients. *Clin. Infect. Dis. Off. Publ. Infect. Dis. Soc. Am.* ciab465.
36. Laczko, D., Hogan, M.J., Toulmin, S.A., Hicks, P., Lederer, K., Gaudette, B.T., Castaño, D., Amanat, F., Muramatsu, H., Oguin, T.H., et al. (2020). A single immunization with nucleoside-modified mRNA vaccines elicits strong cellular and humoral immune responses against SARS-CoV-2 in mice. *Immunity* 53, 724–732.e7.